Title: Allometry of fine roots in forest ecosystems

Authors: Guangshui Chen, Sarah E. Hobbie, Peter B. Reich, Yusheng Yang, David Robinson.

Postal addresses and email addresses:

Guangshui Chen: Key Laboratory for Subtropical Mountain Ecology (Ministry of Science and Technology and Fujian Province Funded), School of Geographical Sciences, Fujian Normal University, Fuzhou 350007, China. Email: gschen@fjnu.edu.cn.

Sarah E. Hobbie: Department of Ecology, Evolution & Behavior, University of Minnesota, St. Paul, MN 55108, USA. Email: shobbie@umn.edu.

Peter B. Reich: 1Department of Forest Resources, University of Minnesota, St. Paul, MN 55108, USA. 2Hawkesbury Institute for the Environment, Western Sydney University, Penrith, New South Wales 2753, Australia. Email: preich@umn.edu.

Yusheng Yang: Key Laboratory for Subtropical Mountain Ecology (Ministry of Science and Technology and Fujian Province Funded), School of Geographical Sciences, Fujian Normal University, Fuzhou 350007, China. Email: geoyys@fjnu.edu.cn.

David Robinson: Institute of Biological & Environmental Sciences, School of Biological Sciences, University of Aberdeen, Aberdeen AB24 3UU, UK. Email: david.robinson@abdn.ac.uk .

Running-title Allometry of fine roots.

Keywords Allometric scaling, carbon allocation, carbon cycle, fine roots, forest ecosystems, net primary production, pipe model

Type of article: Letters

Number of words in the abstract: 148

Number of words in main body of the paper: 4946

Number of references: 73

Number of Figures: 6

Corresponding author: Guangshui Chen (School of Geographical Sciences, Fujian Normal University, 32 Shangsan Rd., Cangshan District, Fuzhou 350007, China. Tel: +86 591 83483731; Fax: +86 591 83465397; Email: gschen@fjnu.edu.cn.). Yusheng Yang (School of Geographical Sciences, Fujian Normal University, 32 Shangsan Rd., Cangshan District, Fuzhou 350007, China. Tel: +86 591 83483731; Fax: +86 591 83465397; Email: geoyys@fjnu.edu.cn.).

Statement of authorship:

All authors designed the study. GC assembled and collected the data. GC and DR conducted data analysis. GC wrote the first draft of the manuscript, and all authors contributed substantially to revisions.

Statement of data accessibility:

We confirm that, should the manuscript be accepted, the data supporting the results will be archived in an appropriate public repository such as Dryad or Figshare and the data DOI will be included at the end of the article.

Abstract

Theoretical predictions regarding fine root production are needed in many ecosystem models but are lacking. Here, we expand the classic pipe model to fine roots and predict isometric scaling relationships between leaf and fine root biomass and among all major biomass production components of individual trees. We also predict that fine root production scales more slowly against increases in leaf production across global forest ecosystems at the stand level. Using meta-analysis, we show fine root biomass scales isometrically against leaf biomass both at the individual tree and stand level. However, despite isometric scaling between stem and coarse root production, fine root production scales against leaf production with a slope of about 0.8 at the stand level, which probably results from more rapid increase of turnover rate in leaves than in fine roots. These analyses help to improve our understandings of allometric theory and controls of belowground C processes.

Key words:

Allometric scaling, belowground carbon allocation, carbon cycle, fine roots, forest ecosystems, net primary production, pipe model.

INTRODUCTION

Fine roots are traditionally defined as being ≤ 2 mm in diameter, short-lived, non-woody, and functionally distinct from coarse roots. Although more nuanced views of fine root classifications exist (McCormack *et al.* 2015b), global data for the historically-defined 'fine root' category are far more abundant and remain useful for evaluating fundamental questions about resource allocation among plant tissues. Along with the hyphae of mycorrhiza-forming fungi that usually colonise them, fine roots are responsible for water and nutrient uptake by plants. Annually, between 10 and 60 % of net primary productivity and gross primary productivity (NPP, GPP; for abbreviations, see Table S1 in Supporting Information) (Jackson *et al.* 1997; Silver & Miya 2001; Ruess *et al.* 2003; Chen *et al.* 2013; McCormack *et al.* 2015c) in terrestrial ecosystems can be cycled through fine roots. Fine-root turnover represents a major pathway of carbon (C) and nutrient flow from plants to soil and is fundamental to both forest NPP and soil C sequestration (Strand et al. 2008).

It is essential to accurately simulate fine root production in ecosystem models such as CBM-CFS2 (Li et al. 2003) and BGC (Pietsch et al. 2005). Such models are hindered by incomplete understanding of fine root dynamics and use simplifications of this critical belowground flux (Jackson *et al.* 2000; Woodward & Osborne 2000; Chapin *et al.* 2009; Iversen 2010; McCormack *et al.* 2013; Chen *et al.* 2014; McCormack *et al.* 2015c). Uncertainty about these fluxes (Lu *et al.* 2012; McCormack *et al.* 2015a) clouds our ability to detect possible positive feedbacks

between the soil C cycle and planetary warming (Cox *et al.* 2000; Friedlingstein *et al.* 2006; Bond-Lamberty & Thomson 2010).

Such a knowledge gap is partly attributable to the labor-intensive nature and methodological difficulty in quantifying fine root variables (e.g., biomass, production and turnover). Interest is growing in developing indirect methods to allow fine root variables to be estimated using data on easily measurable stand and site variables. Large data compilations allow development of allometric equations relating the proportionality of standing biomass and C fluxes to leaves, stem and roots (Reich *et al.* 2014a; Falster *et al.* 2015; Poorter *et al.* 2015; Paul *et al.* 2016). Although a relationship between the surface areas of roots and leaves has been hypothesized based on hydraulic architecture (Davi *et al.* 2009), fine roots are largely neglected by allometric scaling studies. Theoretically explicit allometries of fine roots have yet to be developed.

Forest NPP has been extensively quantified at the stand level; practically, fine root production, and sometimes leaf production, can be estimated in the field only at that level. But, studies on allometric scaling among NPP components have focused primarily on individual trees (e.g., Niklas & Enquist 2001; Niklas & Enquist 2002a; Niklas & Enquist 2002b; Wolf *et al.* 2010), and only a few at the stand level (Litton *et al.* 2007; Malhi *et al.* 2011; Chen *et al.* 2013; Jenkins & Pierce 2016). Yet, allometric scaling relationships at the stand level could be useful for better understanding forest C cycling. For example, operational monitoring of site-level NPP is now underway

using imagery from the satellite-borne techniques across large regions (Turner *et al*. 2005), from which estimates of NPP components could be derived if there were predictable allometric relationships among forest NPP components.

In this study, we first establish theoretical scaling relationships among major components of individual tree NPP based on the classical pipe model (Shinozaki *et al.* 1964); then we explain how these scaling relationships would be expected to change when scaled up to the stand level. Finally, we tested these scaling relationships by assembling several datasets on fine root biomass and production across global forests.

MATERIALS AND METHODS

Theoretical allometric scaling at the individual tree level

The pipe model (Shinozaki *et al*. 1964) was devised to explain consistent linear relationships between the mass of tree leaves and non-photosynthetic tissues with tree height. Such relationships would arise if units of foliage are supported by a certain number of identical units of conductive tissue, or pipes. This geometrical analogy can, in principle, also be extended to roots. In an individual tree, stems, branches and roots can be considered as assemblages of unit pipes (Fig. 1), connected to terminal organs aboveground (leaves) and belowground (fine root modules), with the numbers of pipes decreasing at each branching level. An individual leaf or fine root module is each assumed to be supplied by an equal number of xylem tubes, and is size-invariant in individual traits (i.e., surface area, mass of an individual leaf or fine root module are assumed not to vary with plant size). A fine root module is a dynamic, ephemeral

root terminal structure responsible for uptake of soil nutrients and water. Unlike leaves, which are distinct organs, fine root modules here can be defined on a root diameter basis (e.g., <2mm in diameter), or on a root function basis (e.g., the first two or three root orders), and may also include mycorrhizal fungi and root exudates, in both of which plants invest resources in exchange for nutrients (McCormack *et al.* 2015c). This model should apply both to angiosperms (with xylem vessels) and gymnosperm (with tracheids).

As water is transported through roots to leaves via the tubes, we can assume that, for an individual tree, the number of leaves (n_{fl}) scales isometrically against the number of fine root modules (n_{fr}) to ensure conservation of mass flow through plants spanning a wide range of sizes, such that:

$$n_{fl} \propto n_{fr} \quad (1)$$

The total surface areas of leaves and fine root modules of an individual tree (i.e., sa_{fl} and sa_{fr}), and the total masses of leaves and fine root modules of an individual tree (i.e., m_{fl} and m_{fr}) can be calculated as:

$$sa_{fl} = la_{fl}\, n_{fl} \quad (2)$$

$$sa_{fr} = ra_{fr}\, n_{fr} \quad (3)$$

$$m_{fl} = lw_{fl}\, n_{fl} \quad (4)$$

$$m_{fl} = rw_{fr}\, n_{fr} \quad (5)$$

where la_{fl} and lw_{fl} are the surface area and mass of an individual leaf, and ra_{fr} and rw_{fr} represent the surface area and mass of an individual fine root module, respectively.

144 If traits of an individual leaf or an individual fine root module (i.e., la_{fl} and lw_{fl}, and
145 ra_{fr} and rw_{fr}) are assumed size-invariant, then:
146 $n_{fl} \propto sa_{fl} \propto m_{fl}$ (6)
147 $n_{fr} \propto sa_{fr} \propto m_{fr}$ (7)
148 By combining equations (1) to (7), we can predict the following isometric scaling
149 relationships between leaves and fine-roots:
150 $sa_{fl} \propto sa_{fr}$ (8)
151 $m_{fl} \propto m_{fr}$ (9)
152 The annual leaf and fine root production of an individual plant ($iNPP_{fl}$ and $iNPP_{fr}$)
153 can be written as:
154 $iNPP_{fl} = m_{fl}\, k_{fl}$ (10)
155 $iNPP_{fr} = m_{fr}\, k_{fr}$ (11)
156 where k_{fl} and k_{fr} are annual leaf and fine-root turnover rates, respectively.
157 If we further assume both k_{fl} and k_{fr} are also size-invariant, by combining equations
158 (9) to (11), we can predict isometric scaling between leaf and fine-root production by
159 an individual tree:
160 $iNPP_{fl} \propto iNPP_{fr}$ (12)
161 According to Niklas & Enquist (2002a) and Niklas & Enquist (2002b) the following
162 scaling relationships hold:
163 $iNPP_{st} \propto iNPP_{cr} \propto iNPP_{fl}$ (13)
164 $iTNPP \propto iNPP_{fl}$ (14)

and

$$iNPP_{nl} \propto iNPP_{fl} \quad (15)$$

where $iNPP_{st}$, $iNPP_{cr}$, iTNPP and $iNPP_{nl}$, are the stem production, coarse root production, total production, and non-leaf production, respectively, by an individual tree. Here, we assume root growth rate in Niklas & Enquist (2002a) and Niklas & Enquist (2002b) is equivalent to coarse root production.

Therefore, along a tree size gradient across species (evolutionary scales), we predict the following isometric scaling relationships among all plant organs:

$$iNPP_{fr} \propto iNPP_{fl} \propto iNPP_{st} \propto iNPP_{cr} \propto iNPP_{nl} \quad (16)$$

Allometric scaling at the stand level

Besides plant size, a series of factors, including phylogeny, ontogeny, resource availability, competition, and climate, can affect partitioning of NPP (Clark *et al.* 2001; Gower *et al.* 2001; Litton *et al.* 2007; Chen *et al.* 2013; Malhi *et al.* 2016), and influence relationships among NPP components (i.e., the slopes of the arrows in Fig. 2) and how they deviate from those driven by variation in size.

The predominant drivers of variation in NPP may differ between the individual tree level and the stand level. This difference could affect the partitioning of NPP and generate different scaling relationships among NPP components between the individual tree level and the stand level (Fig. 3). The variation in total NPP of an individual tree (iTNPP) and its components are predominantly controlled by plant size (Fig. 3a,c), which can vary >10-orders of magnitude in terms of biomass (Poorter *et al*.

186 2015) and >8-orders of magnitude in terms of annual growth rates (Niklas & Enquist
187 2002b). As a consequence of such large variation, the effects of factors such as
188 resource supply likely are relatively small. At the individual level, the partitioning of
189 iTNPP among components (or the slope of the log-log bivariate plot) is then expected
190 to be determined predominantly by size-related scaling relationships (Fig. 3a).

191 In forest stands, stem density generally decreases with increasing tree size; the
192 effects of stem density and tree size on total NPP of a stand (TNPP) should therefore
193 counteract each other, making TNPP less dependent on tree size. By contrast, TNPP
194 might be controlled more by other factors such as resource availability and climate
195 (Fig. 3b). Thus, the partitioning of TNPP among components (or slopes of the log-log
196 bivariate plots) at the stand level is likely to be determined predominantly by
197 resource- or climate-related scaling relationships (Fig. 3b). If one standardizes tree
198 size (in the section above about individual tree scaling), the same predictions would
199 occur.

200 From tropical to boreal forests, we expect a general trend of increasing partitioning
201 of TNPP belowground with the decreasing ratio of available N: phosphorous (P) in
202 soil across that biogeographical gradient. This is because the C cost of N acquisition
203 in boreal forests is 13 times greater than in tropical forests, while the C cost of P
204 acquisition in tropical forests is only twice that in boreal forests (Gill & Finzi 2016).
205 We posit non-isometric scaling relationships between fine roots and leaves (more
206 specifically, with a slope less than unity) in terms of stand biomass or production

across global forests, in contrast to the prediction of isometric scaling at the individual level. However, such adjustments in partitioning might be only slight among structural components (i.e., stems and coarse roots) (Fig. 3c,d), due to biomechanical constraints (e.g., trees need to maintain their mechanical balance above- and belowground and require relatively conserved proportions between stems and coarse roots) (Niklas & Spatz 2006). Accordingly, we would expect isometric scaling between stems and coarse roots both at the individual tree and stand level.

Data sets

To estimate the allometric scaling relationships between leaf and fine root biomass at the individual tree level, we extracted data for biomass of fine roots (m_{fr}) and leaves (m_{fl}) of individual trees from the BAAD data set (n=1669) (Falster et al. 2015)(Table S2). The BAAD is suitable for analysis at the individual level in the present study, because measurements were made explicitly on individuals rather than derived as averages using stem density, and biomass was estimated directly rather than by allometric equations (Falster *et al.* 2015) (Table S3). The BAAD data cover a diverse taxa (94 species, 43 family), with tree height of 0.01-32.4 m, diameter of stem at base of 0.05-27.4 cm and total tree mass of 0.000024-1369 kg. However, they come from only 16 studies and are skewed toward seedlings: 80% of the total plant mass data (n=1328) are less than 0.161 kg.

There were three data sources for analysis of scaling relationships at the stand level (Dataset listed in Table S4). The FLUXNET database (Luyssaert *et al*. 2007) is the

main source of NPP and biomass data used in this analysis, including fine root (M_{fr}) and leaf mass (M_{fl}), fine root (NPP_{fr}), leaf (NPP_{fl}), stem (NPP_{st}), coarse root (NPP_{cr}) and woody production (NPP_{wd}), and total production (TNPP) of a stand. Boreal and especially temperate forests are well represented in this database, but tropical forests relatively underrepresented. For this reason we added data on tropical forest NPP components and biomass from Malhi *et al*. (2011) and from the TropForC-db (Anderson-Teixeira *et al*. 2016). The final dataset included 232 forest sites, where at least one of the following data pairs was available: M_{fr} vs. M_{fl}, M_{fr} vs. NPP_{fr}, and NPP_{fr} vs. NPP_{fl}. It covers wide geographic and climatic range: mean annual temperature (MAT) varied from −9.0 to 28.2 °C and mean annual precipitation (MAP) from 271–4500 mm (Table S4).

Total belowground C flux (TBCF) is calculated based on belowground C balance (Ryan *et al.* 2004; Litton *et al.* 2007), i.e., soil CO_2 efflux minus C inputs from aboveground litterfall plus any changes in C stored in roots, litter, and soil C pools, and so is independent of NPP_{fr} estimates. TBCF includes production and respiration of fine and coarse roots, root exudates and mycorrhizae, and can serve as the theoretical upper limit of NPP_{fr} (Nadelhoffer & Raich 1992). TBCF data and the accompanied NPP_{fl} data were extracted from Litton *et al*. (2007). Only TBCF estimates calculated based on the belowground C balance method were selected.

Data analyses

Because NPP_{fr} is usually estimated at the stand level, we did not intend to test the isometric scaling relationships between fine root production and other NPP components at the individual tree level directly, in order to avoid the problem of spurious correlation arising from averaging (i.e., if individual attributes are determined by dividing stand variables by stem density). Instead, only scaling relationships between fine root and leaf biomass both at the individual tree and stand level, and among NPP components at the stand level, were tested in the present study.

All data were $\log_{10}$-transformed to ensure normality and to allow nonlinearity. Because functional rather than predictive relationships were sought for the associations between fine root and leaf biomass and among NPP components, the reduced major axis (RMA; Model Type II) regression was conducted using the form: $\log(y)=\log(a)+\beta \log(x)$, where y and x represent biomass or an NPP component, α is a constant and β the scaling exponent. Differences in RMA slopes were evaluated by likelihood ratio tests (Warton *et al*. 2006). For the BAAD data, the RMA slopes between m_{fr} and m_{fl} were further tested for the combinations of tree species and growing conditions in each study (each study has just one root diameter definition), so that various confounding factors potentially affecting the scaling relationships are assessed (Table S5). Various techniques were used to estimate NPP_{fr} in the compiled dataset (Table S6). In practice NPP_{fr} is likely underestimated because of methodological limitations (Robinson 2004). To assess how this underestimation might impact on allometric scaling, we also compared the slopes of NPP_{fr} vs. NPP_{fl}

regression with TBCF vs. NPP_{fl} regression. A lower slope of NPP_{fr} vs. NPP_{fl} than that of TBCF vs. NPP_{fl} would be consistent with an increasing underestimation of NPP_{fr} in more productive stands.

As direct estimates of k_{fr} and k_{fl} are lacking in these data sets, we calculated the NPP_{fl}/M_{fl} and NPP_{fr}/M_{fr} ratios as respective surrogates for k_{fr} and k_{fl}. The outliers, defined as any datum > 1.5 interquartile ranges below the first quartile or above the third quartile, were discarded. The NPP_{fl}/M_{fl} and NPP_{fr}/M_{fr} ratios were then linearly regressed against TNPP, MAT and MAP to reflect relative changes in leaf and fine root turnover rates across global forests. Differences in the regression between leaves and fine roots were examined by a common slope test.

All the RMA regressions and the common slope tests were performed using SMATR version 2.0 (Warton *et al*. 2006). All the other analyses were done in SPSS 17.0 (SPSS Inc., Chicago, Illinois).

RESULTS

As both m_{fl} and m_{fr} in the BAAD data range in magnitude by nearly 8 orders of magnitude (Fig. 4a), variations in m_{fl} and m_{fr} are undoubtedly predominantly controlled by tree size. The RMA regressions show that there is isometric scaling between m_{fl} and m_{fr} along this size gradient (Fig. 4a; Table S7). Of the 16 combinations of species and growing conditions with significant RMA slopes ($P<0.05$, $n\geq20$) (Table S5), 10 have RMA slopes indistinguishable from unity. Of 7 combinations comprising seedlings, 6 have RMA slopes indistinguishable from unity,

290 and the other one has a near-isometric slope (slope=0.9109) (Table S5). Since the fine
291 root mass of seedlings can probably be estimated more accurately than for mature
292 trees, these results indicated that leaf mass scales isometrically or near-isometrically
293 against fine root mass within a specie at the individual tree level, at least in seedlings.
294 Interestingly, fine root biomass also scales isometrically with leaf biomass at the stand
295 level (Fig. 4b; Table S7), indicating that the isometric scaling between leaf and fine
296 root biomass is quite conservative both at the individual and stand levels. At the stand
297 level, NPP_{fr} scales against NPP_{fl} with a slope (0.794) significantly below unity (Fig.
298 5a; Table S8); there is, however, isometric scaling between NPP_{cr} and NPP_{st} (Fig. 5b;
299 Table S8). This indicates a shift in partitioning from fine roots to leaves, with
300 increasing TNPP. The non-leaf production of a stand (NPP_{nl}) also scales against NPP_{fl}
301 with a slope significantly less than unity (Fig. 5c; Table S8), indicating a decreasing
302 return of biomass production with increasing investment in leaves.

303 TBCF scales against NPP_{fl} with a slope of 0.793, not significantly different from
304 the slope of NPP_{fr} vs. NPP_{fl} (Fig.5a; Table S8). As TBCF serves as an upper limit for
305 NPP_{fr}, the similarity in slope between these two regressions implies that the
306 lower-than-unity scaling of NPP_{fr} vs. NPP_{fl} is unlikely to be an artifact of greater
307 underestimation of NPP_{fr} with increasing TNPP. The comparison of scaling slopes of
308 NPP_{fr} vs. NPP_{fl} and M_{fr} vs. M_{fl} implies that the slower-than-unity scaling of NPP_{fr} vs.
309 NPP_{fl} is also unlikely to be caused by the increasing underestimation of fine root
310 biomass with increasing individual tree size.

For evergreen forests, the NPP_{fl}/M_{fl} and NPP_{fr}/M_{fr} ratios, as respective indicators of leaf and fine root turnover rates, both show significant and positive relations with MAT (Fig. 6a,b; Table S9), but only the NPP_{fl}/M_{fl} ratio has positive relationships with MAP and TNPP (Fig. 6c; Table S9). For deciduous forests, both the NPP_{fl}/M_{fl} and NPP_{fr}/M_{fr} ratios have positive relationships with TNPP, but only the NPP_{fl}/M_{fl} ratio increases with increasing MAT (Fig. 6a; Table S9). In evergreen forests, the NPP_{fl}/M_{fl} ratio tends to increase more rapidly than the NPP_{fr}/M_{fr} ratio with increasing MAP (marginally significant; P=0.109). This indicates a more rapid increase in leaf turnover rate than in fine root turnover rate, which might be the main cause of the slower-than-unity scaling of NPP_{fr} vs. NPP_{fl}.

DISCUSSION

Scaling relationship between fine root and leaf biomass

The isometric scaling relationships between leaf and fine root biomass both at the individual tree and the stand levels validate our prediction of the extended pipe model. It indicates that trees are constrained to maintain a common hydraulic architecture and functions, i.e., a hydraulic continuum from fine roots to leaves (Shinozaki *et al.* 1964; Magnani *et al.* 2000). Some studies have also reported a linear relationship between fine root and leaf biomass for several coniferous species, e.g., Santantonio (1989) and Vanninen & Makela (1999). Fine root biomass was also positively correlated with stand basal area (Vanninen & Makela 1999; Helmisaari *et al.* 2007; Finér *et al.* 2011b; Lehtonen *et al.* 2016). In a study by Cermak & Nadezhdina (2011), absorbing root

surface area was related linearly to the basal area of individuals across almost 500 trees of 11 woody species of different ages, sizes, and growing conditions. As basal area is predicted to be proportional to leaf area (Shinozaki *et al.* 1964; West *et al.* 1999), this also implies linear relationships between absorbing root surface area and leaf area of an individual. These results suggest that the pipe model can be successfully extended to fine roots.

The core assumption of our extended pipe model is that both the above- and belowground terminal units of this tube structure are size-invariant. However, the belowground structural analog to the leaf is still under debate (Pregitzer 2008). Traditionally, fine roots have been defined as those <2 mm in diameter; in some cases smaller (e.g. 1.0 mm or even 0.5 mm) or larger (e.g. 5.0 mm) diameter cutoffs are also used (Helmisaari *et al.* 2009; Finér *et al.* 2011b; McCormack *et al.* 2015c). However, this approach has been criticized for not accounting for the heterogeneity in both the forms and functions of fine roots (Pregitzer *et al.* 2002; Guo *et al.* 2008). New definitions of fine roots are emerging based on their functional heterogeneity, by which fine roots are grouped into individual root orders or separated into shorter-lived fibrous roots and longer-lived transport roots (Guo *et al.* 2008; McCormack *et al.* 2015c). However, the diameter-based definition was used in most of the current data on fine roots (Finér *et al.* 2011a; Yuan & Chen 2012a). We argue that this definition does not undermine our assumption that individual fine root units are size-invariant: as seen in Table S5, there was no systematic difference in RMA slopes among

different root diameter definitions. This assumption would be reasonable for deriving predictions, provided that the size-dependence for total fine root mass is large relative to size-dependent changes in individual fine root traits. Indeed, the branch architecture, morphology, anatomy, and physiology of the fine root systems seem to be relatively conserved within a species (Pregitzer *et al.* 2002; Kembel & Cahill 2005; Guo *et al.* 2008). In future, however, it will be valuable to have estimates based on an explicit definition of fine roots in terms of function (McCormack *et al.* 2015c) to further verify scaling relationships described here.

Although our extended pipe model predicts scaling relationships between fine roots and leaves based primarily on hydraulic architecture, it is sufficiently flexible to include adaptive responses of roots to nutrient availability, by accounting for variations in construction (e.g., rw_{fr}) and maintenance (e.g., k_{fr}) costs associated with an individual fine root module (Yuan & Chen 2010; Yuan & Chen 2012a).

Scaling relationships among NPP components at the stand level

Although isometric scaling relationships among all NPP components are predicted at the individual level (equation (16)), a test of this prediction awaits the compilation of enough data on fine root production estimated explicitly at the individual level. To our knowledge, this study is the first to explore allometric scaling relationships among NPP components across global forest ecosystems at the stand level. Such relationships could help to better constrain estimates of forest C balance across broad spatial scales.

373 At the stand level, we found NPP_{fr} lags behind NPP_{fl} with a slope lower than unity,
374 which echoes previous syntheses, e.g., Litton *et al*. (2007) who found that partitioning
375 of GPP to TBCF decreased with increasing GPP across 34 forest sites; and Yuan &
376 Chen (2012a) who reported that the average increases in fine root production are
377 generally smaller than those of aboveground NPP with greater soil nutrients along
378 global nutrient gradients or in nutrient addition experiments. These results show that
379 above- and belowground productivities are coupled across climatic or nutrient
380 gradients, but production shifts from belowground to aboveground with increasing
381 productivity. The highest productivity sites in our synthesis came from low latitude
382 sites. This supports the hypothesis proposed by Gill & Finzi (2016) that the main
383 limitation on forest productivity changes from belowground at high latitudes to
384 aboveground at low latitudes.

385 Isometric scaling between woody components (i.e., NPP_{st} and NPP_{cr}) at the stand
386 level is consistent with patterns seen at the individual scale (Niklas & Enquist 2002a;
387 Niklas & Enquist 2002b). This may be due to the need for structural organs to
388 maintain mechanical stability, e.g., wind-induced bending moments exerted at the
389 stem base are balanced by a counter-resisting moment generated by the root system to
390 prevent windfall (Niklas & Spatz 2006). Hence, partitioning between structural organs
391 would be less affected by resource availability or climate.

392 Some studies have shown that NPP_{fl} (or litterfall, a proxy of NPP_{fl}) is a fixed
393 proportion or log-linearly related to TNPP among stands across a specific biome

394 (Clark *et al.* 2001; Malhi *et al.* 2011). However, we show that there is
395 lower-than-unity slope for NPP_{nl} vs. NPP_{fl} scaling at the stand level across global
396 forests, which is different from the isometric scaling between iTNPP vs. $iNPP_{fl}$ or
397 between $iNPP_{nl}$ vs. $iNPP_{fl}$ at the individual level (Niklas & Enquist 2002b). This
398 probably indicates a reduced return of woody biomass production on increasing leaf
399 investment at higher NPP sites due to increased light competition. However, this does
400 not exclude the possibility that greater efficiency of production per unit leaf would
401 occur at higher NPP when in fertile sites, good climate, and or with fast-producing
402 species. However, allometric scaling cannot allow us to distinguish between those two
403 mechanistic possibilities. Nevertheless, our results imply that NPP_{fl} cannot be used
404 reliably as an invariant proportion of TNPP across global forests.

405 **Why does NPP_{fr} lag behind NPP_{fl} ?**

406 NPP components depend not only on biomass, but also on turnover rates. Because M_{fr}
407 scales isometrically with M_{fl}, the lower-than-unity slope for NPP_{fr} vs. NPP_{fl} at the
408 stand level would arise from either increasing underestimation of NPP_{fr} in higher NPP
409 contexts, or more rapid increase in the turnover rate of leaves than fine roots with
410 increasing stand productivity.

411 Unlike fine root biomass, which can be quantified relatively well by the coring
412 method if sample size is sufficient to overcome high spatial heterogeneity (Vogt *et al.*
413 1998; Park *et al.* 2007), estimating fine root production is more challenging (Finér *et*
414 *al*. 2011b). Both direct (minirhizotrons, ingrowth cores, sequential soil coring) and

415 indirect methods (C and N budgets, isotopic approaches) have been used, each with
416 its respective advantages and disadvantages (Vogt *et al.* 1998; Majdi *et al.* 2005;
417 Hendricks *et al.* 2006; Withington *et al.* 2006; Strand *et al.* 2008; Yuan & Chen
418 2012b). NPP_{fr} estimates differ significantly among methods when used at the same
419 sites (Hendricks *et al.* 2006; Withington *et al.* 2006; Yuan & Chen 2012b), and no
420 single method is superior. TBCF calculated by soil C balance is currently the 'gold
421 standard' that provides the most reliable estimates of total root C allocation (Giardina
422 & Ryan 2002; Litton *et al.* 2007) and which can serve as the upper-limit constraint on
423 NPP_{fr} (Nadelhoffer & Raich 1992). Comparing the difference in intercepts of TBCF
424 and NPP_{fr} scaling against NPP_{fl} indicates that on average nearly 20 percent of TBCF
425 goes to fine root production globally, which is lower than the estimate (1/3 of TBCF)
426 suggested by Nadelhoffer & Raich (1992) based on N budgets. However, the
427 similarity of the two slopes indicates that underestimation of NPP_{fr} may occur, but
428 probably affects only the intercept of the regression rather than the slope. The most
429 plausible explanation for the lower-than-unity slope for NPP_{fr} vs. NPP_{fl} is that leaf
430 and fine root turnover change at different rates with increasing NPP. Although we
431 assume that both k_{fr} and k_{fl} are size-invariant, it is likely that k_{fr} and k_{fl} both vary
432 along global environmental gradients (Reich *et al.* 2014a).

433 For evergreen forests, both the NPP_{fl}/M_{fl} and NPP_{fr}/M_{fr} ratios, and for deciduous
434 forests, the NPP_{fl}/M_{fl} ratio, increased with MAT, as found in some previous studies
435 (Gill & Jackson 2000; Yuan & Chen 2010; Finér *et al.* 2011b; Reich *et al.* 2014b).

For example, using a database of 190 studies, Gill & Jackson (2000) found fine root turnover rates increased exponentially with MAT for grasslands and forests. Reich et al. (2014b) reported that across 127 sites along a 2,160-km gradient in North America, needle lifespans of four dominant evergreen conifers increased with decreasing MAT. Increases in tissue maintenance cost, N mineralization, and the pathogen and herbivore pressures associated with warmer and wetter conditions are possible causes of these relationships (Eissenstat *et al.* 2000; Gill & Jackson 2000; Finér *et al.* 2011b).

So far, however, no study has compared the relative changes in k_{fr} and k_{fl} along environmental gradients. We found that, for evergreen forests, the slope of NPP_{fl}/M_{fl} ratio vs. MAP was higher than that of NPP_{fr}/M_{fr} ratio vs. MAP (P=0.109), indicating that leaf turnover rates probably increase more rapidly than fine root turnover rates along the MAP gradient. This might arise if increases in annual precipitation cause more green leaf litter production and increase leaf turnover aboveground, with no corresponding effects belowground.

Why is there an isometric scaling relationship between M_{fl} and M_{fr} and between m_{fl} and m_{fr}, but a non-isometric scaling relationship between NPP_{fl} and NPP_{fr}? An explanation is that plants may regulate biomass distribution between leaves and fine roots simply on the basis of the proportion of leaves and fine roots required to maintain current functions, as predicted by the extended pipe model, while the allocation of C is adjusted to maintain this proportionality between leaves and fine roots, given differences in turnover rates. This mechanism is consistent with pruning

457 experiments demonstrating that both leaves and roots of herbs quickly recovered to
458 their original biomass fractions after the leaf or root mass was halved (Brouwer 1963;
459 Poorter & Nagel 2000).

460 In conclusion, we have expanded the pipe model to fine roots, and showed how
461 scaling exponents change from the individual tree to the stand level. These results
462 help advance understanding of allometry theory, and provide new insights into the
463 patterns and controls of belowground C processes, which are largely neglected by
464 existing C allocation studies. The allometric relationships between fine roots and
465 other components revealed here may serve as robust constraints on, or validations of,
466 future measurements and models, and provide new model parameterizations. Future
467 allometry studies should integrate the internal size-driven allometric partitioning
468 process with those driven by the external factors (resources, climate, competition, etc),
469 and focus greater attention at the stand level. More data are also needed to understand
470 the allometry and variation in fine roots among forest stands at the global scale,
471 especially comparing results obtained using functionally defined versus size-based
472 classification of fine roots.

473 **ACKNOWLEDGEMENTS**

474 We thank Chensen Xu for drawing Figure 1. This synthesis benefits directly from
475 different sources of dataset, including the forest flux database (Luyssaert *et al*., 2007),
476 BAAD (Falster *et al*. 2015), ForC-db (https://github.com/forc-db), dataset of Malhi *et*

al. (2011) and Litton *et al*. (2007). We are grateful to all these authors, site investigators and their funding agencies contributing to these dataset. We thank the various regional flux networks (Afriflux, AmeriFlux, AsiaFlux, CarboAfrica, CarboEurope-IP, ChinaFlux, Fluxnet-Canada, KoFlux, LBA, NECC, OzFlux, TCOS-Siberia, USCCC), and the Fluxnet project, for support in obtaining these measurements. We also thank two reviewers for their valuable comments on an earlier version of this paper. This study was supported by the National Natural Science Foundation of China (31422012 and 31830014).

AUTHOR CONTRIBUTIONS

All authors designed the study. GC assembled and collected the data. GC and DR conducted data analysis. GC wrote the first draft of the manuscript, and all authors contributed substantially to revisions.

DATA ACCESSIBILITY STATEMENT

All data used in this analysis are tabulated in the Supporting Information.

REFERENCES

Anderson-Teixeira, K.J., Wang, M.M.H., McGarvey, J.C. & LeBauer, D.S. (2016). Carbon dynamics of mature and regrowth tropical forests derived from a pantropical database (TropForC-db). *Global Change Biology*, 22, 1690.

498 Bond-Lamberty, B. & Thomson, A. (2010). Temperature-associated increases in the
499 global soil respiration record. *Nature*, 464, 579-582.
500 Brouwer, R. (1963). Some aspects of the equilibrium between overground and
501 underground plant parts. *Jaarboek van het Instituut voor Biologisch en*
502 *Scheikundig onderzoek aan Landbouwgewassen*, 1963, 31–39.
503 Cermak, J. & Nadezhdina, N. (2011). Field Studies of Whole-Tree Leaf and Root
504 Distribution and Water Relations in Several European Forests. In: *Forest*
505 *Management and the Water Cycle* (eds. Bredemeier, M, Cohen, S, Godbold,
506 DL, Lode, E, Pichler, V & Schleppi, P). Springer Netherlands, pp. 65-88.
507 Chapin, F.S., McFarland, J., McGuire, A.D., Euskirchen, E.S., Ruess, R.W. &
508 Kielland, K. (2009). The changing global carbon cycle: linking plant-soil
509 carbon dynamics to global consequences. *Journal of Ecology*, 97, 840-850.
510 Chen, G., Yang, Y. & Robinson, D. (2013). Allocation of gross primary production in
511 forest ecosystems: allometric constraints and environmental responses. *New*
512 *Phytologist*, 200, 1176-1186.
513 Chen, G., Yang, Y. & Robinson, D. (2014). Allometric constraints on, and trade-offs
514 in, belowground carbon allocation and their control of soil respiration across
515 global forest ecosystems. *Global Change Biology*, 20, 1674-1684.
516 Clark, D.A., Brown, S., Kicklighter, D.W., Chambers, J.Q., Thomlinson, J.R., Ni, J. *et*
517 *al.* (2001). Net primary production in tropical forests: an evaluation and
518 synthesis of existing field data. *Ecological Applications*, 11, 371-384.

519 Cox, P.M., Betts, R.A., Jones, C.D., Spall, S.A. & Totterdell, I.J. (2000). Acceleration
520 of global warming due to carbon-cycle feedbacks in a coupled climate model.
521 *Nature*, 408, 184-187.
522 Davi, H., Barbaroux, C., Francois, C. & Dufrêne, E. (2009). The fundamental role of
523 reserves and hydraulic constraints in predicting LAI and carbon allocation in
524 forests. *Agricultural & Forest Meteorology*, 149, 349-361.
525 Eissenstat, D.M., Wells, C.E., Yanai, R.D. & Whitbeck, J.L. (2000). Building roots in
526 a changing environment: implications for root longevity. *New Phytologist*, 147,
527 33-42.
528 Falster, D.S., Duursma, R.A., Ishihara, M.I., Barneche, D.R., FitzJohn, R.G.,
529 Vårhammar, A. *et al.* (2015). BAAD: a Biomass And Allometry Database for
530 woody plants. *Ecology*, 96, 1445-1445.
531 Finér, L., Ohashi, M., Noguchi, K. & Hirano, Y. (2011a). Factors causing variation in
532 fine root biomass in forest ecosystems. *Forest Ecology and Management*, 261,
533 265-277.
534 Finér, L., Ohashi, M., Noguchi, K. & Hirano, Y. (2011b). Fine root production and
535 turnover in forest ecosystems in relation to stand and environmental
536 characteristics. *Forest Ecology and Management*, 262, 2008-2023.
537 Friedlingstein, P., Cox, P., Betts, R., Bopp, L., von Bloh, W., Brovkin, V. *et al.*
538 (2006). Climate–carbon cycle feedback analysis: results from the C4MIP
539 model intercomparison. *Journal of Climate*, 19, 3337-3353.

Giardina, C.P. & Ryan, M.G. (2002). Total belowground carbon allocation in a fast-growing <i>Eucalyptus</i> plantation estimated using a carbon balance approach. *Ecosystems*, 5, 487-499.

Gill, A.L. & Finzi, A.C. (2016). Belowground carbon flux links biogeochemical cycles and resource-use efficiency at the global scale. *Ecology Letters*, 19, 1419-1428.

Gill, R.A. & Jackson, J.A. (2000). Global patterns of root turnover for terrestrial ecosystems. *New Phytologist*, 147, 13-31.

Gower, S.T., Krankina, O., Olson, R.J., Apps, M., Linder, S. & Wang, C. (2001). Net primary production and carbon allocation patterns of boreal forest ecosystems. *Ecological Applications*, 11, 1395-1411.

Guo, D., Xia, M., Wei, X., Chang, W., Liu, Y. & Wang, Z. (2008). Anatomical traits associated with absorption and mycorrhizal colonization are linked to root branch order in twenty-three Chinese temperate tree species. *New Phytologist*, 180, 673-683.

Helmisaari, H.-S., Ostonen, I., Lõhmus, K., Derome, J., Lindroos, A.-J., Merilä, P. *et al.* (2009). Ectomycorrhizal root tips in relation to site and stand characteristics in Norway spruce and Scots pine stands in boreal forests. *Tree Physiology*, 29, 445-456.

559 Helmisaari, H.S., Derome, J., Nojd, P. & Kukkola, M. (2007). Fine root biomass in
560 relation to site and stand characteristics in Norway spruce and Scots pine
561 stands. *Tree Physiology*, 27, 1493-1504.
562 Hendricks, J.J., Hendrick, R.L., Wilson, C.A., Mitchell, R.J., Pecot, S.D. & Guo, D.
563 (2006). Assessing the patterns and controls of fine root dynamics: an empirical
564 test and methodological review. *Journal of Ecology*, 94, 40-57.
565 Iversen, C.M. (2010). Digging deeper: fine-root responses to rising atmospheric CO2
566 concentration in forested ecosystems. *New Phytologist*, 186, 346-357.
567 Jackson, R.B., Mooney, H.A. & Schulzes, E.-D. (1997). A global budget for fine root
568 biomass, surface area, and nutrient contents. *Proc. Natl. Acad. Sci. USA*, 94,
569 7362–7366.
570 Jackson, R.B., Schenk, H., Jobbagy, E., Canadell, J., Colello, G., Dickinson, R. *et al.*
571 (2000). Belowground consequences of vegetation change and their treatment
572 in models. *Ecological Applications*, 10, 470-483.
573 Jenkins, D.G. & Pierce, S. (2016). General allometric scaling of net primary
574 production agrees with plant adaptive strategy theory and has tipping points.
575 *Journal of Ecology*.
576 Kembel, S.W. & Cahill, J.F. (2005). Plant phenotypic plasticity belowground: A
577 phylogenetic perspective on root foraging trade-offs. *American Naturalist*, 166,
578 216-230.

579 Lehtonen, A., Palviainen, M., Ojanen, P., Kalliokoski, T., Nöjd, P., Kukkola, M. *et al.*
580 (2016). Modelling fine root biomass of boreal tree stands using site and stand
581 variables. *Forest Ecology and Management*, 359, 361-369.
582 Li, Z., Kurz, W.A., Apps, M.J. & Beukema, S.J. (2003). Belowground biomass
583 dynamics in the Carbon Budget Model of the Canadian Forest Sector: recent
584 improvements and implications for the estimation of NPP and NEP. *Canadian*
585 *Journal of Forest Research*, 33, 126-136.
586 Litton, C.M., Raich, J.W. & Ryan, M.G. (2007). Carbon allocation in forest
587 ecosystems. *Global Change Biology*, 13, 2089-2109.
588 Lu, M., Zhou, X., Yang, Q., Li, H., Luo, Y., Fang, C. *et al.* (2012). Responses of
589 ecosystem carbon cycle to experimental warming: a meta-analysis. *Ecology*,
590 94, 726-738.
591 Luyssaert, S., Inglima, I., Jung, M., Richardson, A.D., Reichstein, M., Papale, D. *et al.*
592 (2007). CO2 balance of boreal, temperate, and tropical forests derived from a
593 global database. *Global Change Biology*, 13, 2509-2537.
594 Magnani, F., Mencuccini, M. & Grace, J. (2000). Age-related decline in stand
595 productivity: the role of structural acclimation under hydraulic constraints.
596 *Plant Cell & Environment*, 23, 251–263.
597 Majdi, H., Pregitzer, K., Moren, A.S., Nylund, J.E. & Agren, G.I. (2005). Measuring
598 fine root turnover in forest ecosystems. *Plant and Soil*, 276, 1-8.

599 Malhi, Y., Doughty, C. & Galbraith, D. (2011). The allocation of ecosystem net
600 primary productivity in tropical forests. *Philosophical Transactions of the*
601 *Royal Society B: Biological Sciences*, 366, 3225-3245.
602 Malhi, Y., Girardin, C., Goldsmith, G., Doughty, C., Salinas, N., Metcalfe, D. *et al.*
603 (2016). The variation of productivity and its allocation along a tropical
604 elevation gradient: a whole carbon budget perspective. *New Phytologist*, 214,
605 1019-1032.
606 McCormack, M.L., Crisfield, E., Raczka, B., Schnekenburger, F., Eissenstat, D.M. &
607 Smithwick, E.A.H. (2015a). Sensitivity of four ecological models to
608 adjustments in fine root turnover rate. *Ecological Modelling*, 297, 107-117.
609 McCormack, M.L., Dickie, I.A., Eissenstat, D.M., Fahey, T.J., Fernandez, C.W., Guo,
610 D. *et al.* (2015b). Redefining fine roots improves understanding of
611 below-ground contributions to terrestrial biosphere processes. *New Phytologist*,
612 207, 505-518.
613 McCormack, M.L., Dickie, I.A., Eissenstat, D.M., Fahey, T.J., Fernandez, C.W., Guo,
614 D. *et al.* (2015c). Redefining fine roots improves understanding of
615 belowground contributions to terrestrial biosphere processes. *New Phytologist*,
616 207, 505-518.
617 McCormack, M.L., Eissenstat, D.M., Prasad, A.M. & Smithwick, E.A.H. (2013).
618 Regional scale patterns of fine root lifespan and turnover under current and
619 future climate. *Global Change Biology*, 19, 1697-1708.

620 Nadelhoffer, K.J. & Raich, J.W. (1992). Fine root production estimates and
621 belowground carbon allocation in forest ecosystems. *Ecology*, 73, 1139-1147.
622 Niklas, K.J. & Enquist, B.J. (2001). Invariant scaling relationships for interspecific
623 plant biomass production rates and body size. *Proceedings of the National*
624 *Academy of Sciences*, 98, 2922-2927.
625 Niklas, K.J. & Enquist, B.J. (2002a). Canonical rules for plant organ biomass
626 partitioning and annual allocation. *American Journal of Botany*, 89, 812-819.
627 Niklas, K.J. & Enquist, B.J. (2002b). On the vegetative biomass partitioning of seed
628 pant leaves, stems, and roots. *Anglais*, 159, 482-497.
629 Niklas, K.J. & Spatz, H.-C. (2006). Allometric theory and the mechanical stability of
630 large trees: proof and conjecture. *American Journal of Botany*, 93, 824-828.
631 Park, B.B., Yanai, R.D., Vadeboncoeur, M.A. & Hamburg, S.P. (2007). Estimating
632 Root Biomass in Rocky Soils using Pits, Cores, and Allometric Equations
633 Abbreviations: dbh, diameter at breast height. *Soil Sci. Soc. Am. J.*, 71,
634 206-213.
635 Paul, K.I., Roxburgh, S.H., Chave, J., England, J.R., Zerihun, A., Specht, A. *et al.*
636 (2016). Testing the generality of above-ground biomass allometry across plant
637 functional types at the continent scale. *Global Change Biology*, 22,
638 2106-2124.

639 Pietsch, S.A., Hasenauer, H. & Thornton, P.E. (2005). BGC-model parameters for
640 tree species growing in central European forests. *Forest Ecology &*
641 *Management*, 211, 264-295.
642 Poorter, H., Jagodzinski, A.M., Ruiz-Peinado, R., Kuyah, S., Luo, Y., Oleksyn, J. *et*
643 *al.* (2015). How does biomass distribution change with size and differ among
644 species? An analysis for 1200 plant species from five continents. *New*
645 *Phytologist*, 208, 736-749.
646 Poorter, H. & Nagel, O. (2000). The role of biomass allocation in the growth response
647 of plants to different levels of light, CO₂, nutrients and water: a
648 quantitative review. *Australian Journal of Plant Physiology*, 27, 595-607.
649 Pregitzer, K.S. (2008). Tree root architecture - form and function. *New Phytologist*,
650 180, 562-564.
651 Pregitzer, K.S., DeForest, J.L., Burton, A.J., Allen, M.F., Ruess, R.W. & Hendrick,
652 R.L. (2002). Fine root architecture of nine North American trees. *Ecological*
653 *Monographs*, 72, 293-309.
654 Reich, P.B., Luo, Y., Bradford, J.B., Poorter, H., Perry, C.H. & Oleksyn, J. (2014a).
655 Temperature drives global patterns in forest biomass distribution in leaves,
656 stems, and roots. *Proceedings of the National Academy of Sciences*, 111,
657 13721-13726.
658 Reich, P.B., Rich, Roy L., Lu, X., Wang, Y.-P. & Oleksyn, J. (2014b). Biogeographic
659 variation in evergreen conifer needle longevity and impacts on boreal forest

carbon cycle projections. *Proceedings of the National Academy of Sciences of the United States of America*, 111, 13703-13708.

Robinson, D. (2004). Scaling the depths: below-ground allocation in plants, forests and biomes. *Functional Ecology*, 18, 290-295.

Ruess, R.W., Hendrick, R.L., Burton, A.J., Pregitzer, K.S., Sveinbjornsson, B., Allen, M.E. *et al.* (2003). Coupling fine root dynamics with ecosystem carbon cycling in black spruce forests of interior Alaska. *Ecological Monographs*, 73, 643-662.

Ryan, M.G., Binkley, D., Fownes, J.H., Giardina, C.P. & Senock, R.S. (2004). An experimental test of the causes of forest growth decline with stand age. *Ecological Monographs*, 74, 393-414.

Santantonio, D. (1989). Dry-Matter Partitioning and Fine-Root Production in Forests — New Approaches to a Difficult Problem. In: *Biomass Production by Fast-Growing Trees* (eds. Pereira, JS & Landsberg, JJ). Springer Netherlands, pp. 57-72.

Shinozaki, K., Yoda, K., Hozumi, K. & Kira, T. (1964). A quantitative analysis of plant form – the pipe model theory. I. Basic analysis. *Japanese Journal of Ecology*, 14, 97-105.

Silver, W.L. & Miya, R.K. (2001). Global patterns in root decomposition: comparisons of climate and litter quality effects. *Oecologia*, 129, 407-419.

680 Strand, A.E., Pritchard, S.G., McCormack, M.L., Davis, M.A. & Oren, R. (2008).
681 Irreconcilable differences: Fine-root life spans and soil carbon persistence.
682 *Science*, 319, 456-458.
683 Turner, D.P., Ritts, W.D., Cohen, W.B., Maeirsperger, T.K., Gower, S.T.,
684 Kirschbaum, A.A. *et al.* (2005). Site-level evaluation of satellite-based global
685 terrestrial gross primary production and net primary production monitoring.
686 *Global Change Biology*, 11, 666-684.
687 Vanninen, P. & Makela, A. (1999). Fine root biomass of Scots pine stands differing in
688 age and soil fertility in southern Finland. *Tree Physiology*, 19, 823-830.
689 Vogt, K.A., Vogt, D.J. & Bloomfield, J. (1998). Analysis of some direct and indirect
690 methods for estimating root biomass and production of forests at an ecosystem
691 level. In: *Root Demographics and Their Efficiencies in Sustainable*
692 *Agriculture, Grasslands and Forest Ecosystems*. Springer, pp. 687-720.
693 Warton, D.I., Wright, I.J., Falster, D.S. & Westoby, M. (2006). Bivariate line-fitting
694 methods for allometry. *Biological Reviews*, 81, 259-291.
695 West, G.B., Brown, J.H. & Enquist, B.J. (1999). A general model for the structure and
696 allometry of plant vascular systems. *Nature*, 400, 664-667.
697 Withington, J.M., Reich, P.B., Oleksyn, J. & Eissenstat, D.M. (2006). Comparisons of
698 structure and life span in roots and leaves among temperate trees. *Ecological*
699 *Monographs*, 76, 381-397.

Wolf, A., Field, C.B. & Berry, J.A. (2010). Allometric growth and allocation in forests: a perspective from FLUXNET. *Ecological Applications*, 21, 1546-1556.

Woodward, F. & Osborne, C. (2000). The representation of root processes in models addressing the responses of vegetation to global change. *New Phytologist*, 147, 223-232.

Yuan, Z.Y. & Chen, H.Y.H. (2010). Fine Root Biomass, Production, Turnover Rates, and Nutrient Contents in Boreal Forest Ecosystems in Relation to Species, Climate, Fertility, and Stand Age: Literature Review and Meta-Analyses. *Critical Reviews in Plant Sciences*, 29, 204-221.

Yuan, Z.Y. & Chen, H.Y.H. (2012a). A global analysis of fine root production as affected by soil nitrogen and phosphorus. *Proceedings of the Royal Society B: Biological Sciences*, 279, 3796-3802.

Yuan, Z.Y. & Chen, H.Y.H. (2012b). Indirect methods produce higher estimates of fine root production and turnover rates than direct methods. *Plos One*, 7, e48989.

SUPPORTING INFORMATION

Additional Supporting Information may be downloaded via the online version of this article at Wiley Online Library (www.ecologyletters.com).

724 Figure legends

725

726 Fig. 1 Symbolic representation of branch vascular structure in stems and branches,
727 that end with photosynthetic organs (leaves); and in roots, that end with fine root
728 modules. The lines denote xylem tubes. An individual leaf or an individual fine root
729 module each is assumed supplied by an equal number of xylem tubes, and is
730 size-invariant in individual traits (i.e., surface area, mass). A fine root module is a
731 dynamic, ephemeral terminal root segment responsible for uptake of soil resources,
732 which can be defined on a root diameter basis (e.g., <2mm in diameter) or a root
733 function basis (e.g., the first two or three root orders), and may also include
734 mycorrhizal fungi and root exudates.

735

736 Fig. 2 Conceptual diagram showing different allometric scaling relationships between
737 two log-transformed individual tree NPP components *i* and *j*. The ellipses denote the
738 scatter of data points which represents a sample of forest trees (either within a stand
739 or across stands), and the three grey arrows show the linear regressions of those data.
740 Besides plant size, a series of factors, including ontogeny, competition, resource
741 availabilities, and climate, could affect partitioning of NPP, and force the slope of the
742 relationship between the two individual tree NPP components to deviate from that
743 caused by variation in size (for purposes of illustration, the changes in the direction of
744 this slope caused by these factors shown here are arbitrary).

745

Fig. 3 Conceptual diagrams showing different allometric scaling relationships between $\log_{10}$-transformed components of biomass or production: between fine root and leaf biomass at the individual tree level (a) and the stand level (b); and between coarse roots and stems at the individual tree level (c) and the stand level (d).

The slopes of the grey arrows show the separate effects attributable to size or resources/climate (i.e., temperature and precipitation) on overall partitioning of biomass or production. The ellipses denote the data scatter of a sample of forest sites, and the double-headed red arrows show the linear regressions of these data, with its length showing the order of variation in magnitude.

At the individual tree level, the variations in biomass or production components are dominated by the size effect. At the stand level, the variations are caused predominantly by resource availability or climate (temperature and precipitation), etc. There could then be different exponents for the log-log allometric scaling relationships (i.e., the slopes of the double-headed red arrows) between the individual trees and the stand level.

Compared with structural organs (i.e., coarse roots and stems), the partitioning of biomass or production between short-lived resource-acquisitive components (i.e., leaves and fine roots) might be more responsive to variations in resource availability or climate, i.e., the intersection angles between the two grey arrows is wider in Fig. 3a and Fig. 3b than in Fig. 3c and Fig. 3d.

766 Thus, the discrepancy in the scaling slopes of fine roots vs. leaves from the
767 individual tree level to the stand level is predicted to be much larger than that of
768 coarse roots vs. stems.
769
770 Fig. 4 Reduced major axis regressions of $\log_{10}$ of fine root vs. foliage biomass (a) at
771 the individual level (m_{fr} vs. m_{fl}), and (b) at the stand level (M_{fr} vs. M_{fl}).
772
773 Fig. 5 Reduced major axis (RMA) regressions of $\log_{10}$ components of net primary
774 production of a stand (NPP, in g C m^{-2} yr^{-1}) across global forests: (a) fine root
775 production (NPP_{fr}) vs. foliage production (NPP_{fl}); (b) coarse root production (NPP_{cr})
776 vs. stem production (NPP_{st}); and (c) non-leaf production (NPP_{nl}) vs. NPP_{fl}. RMA
777 regression of $\log_{10}$ total belowground carbon flux (TBCF) vs. NPP_{fl} was also plotted
778 in (a) for comparison with that of NPP_{fr} vs. NPP_{fl}.
779
780 Fig. 6 Ordinary least-squares linear regressions of $\log_{10}$ of the production/biomass
781 ratio of leaves (NPP_{fl}/M_{fl}) and fine roots (NPP_{fr}/M_{fr}) of a stand against $\log_{10}$ of mean
782 annual temperature (MAT) (a, b), and $\log_{10}$ of mean annual precipitation (MAP) (c, d)
783 across the global forests. The parameters of these regressions see Table S9.
784

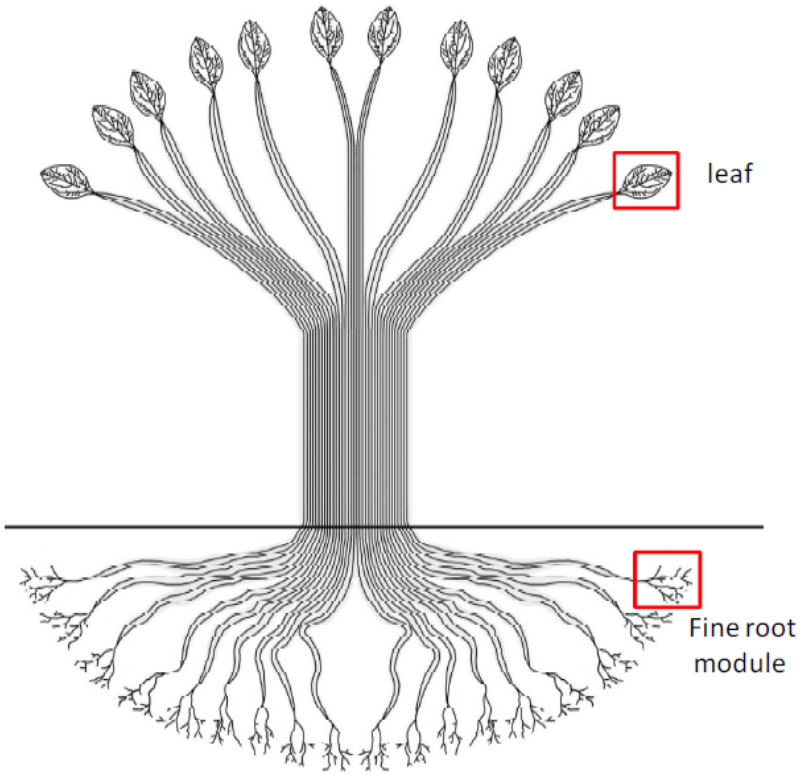

865
866

Fig. 1

785
786 Fig 1
787

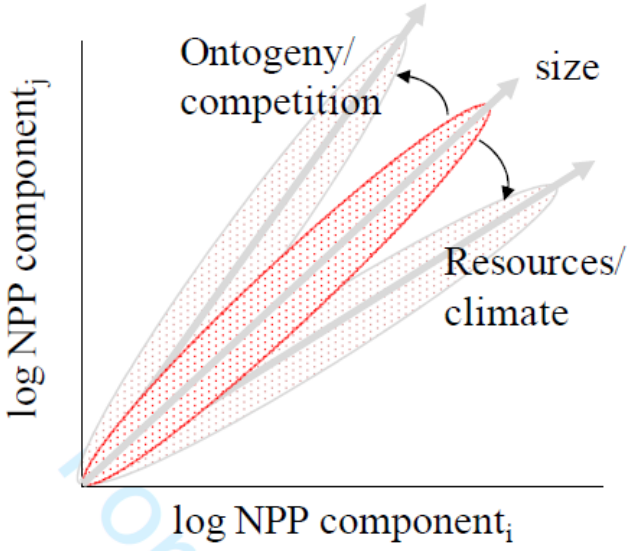

Fig. 2

788
789

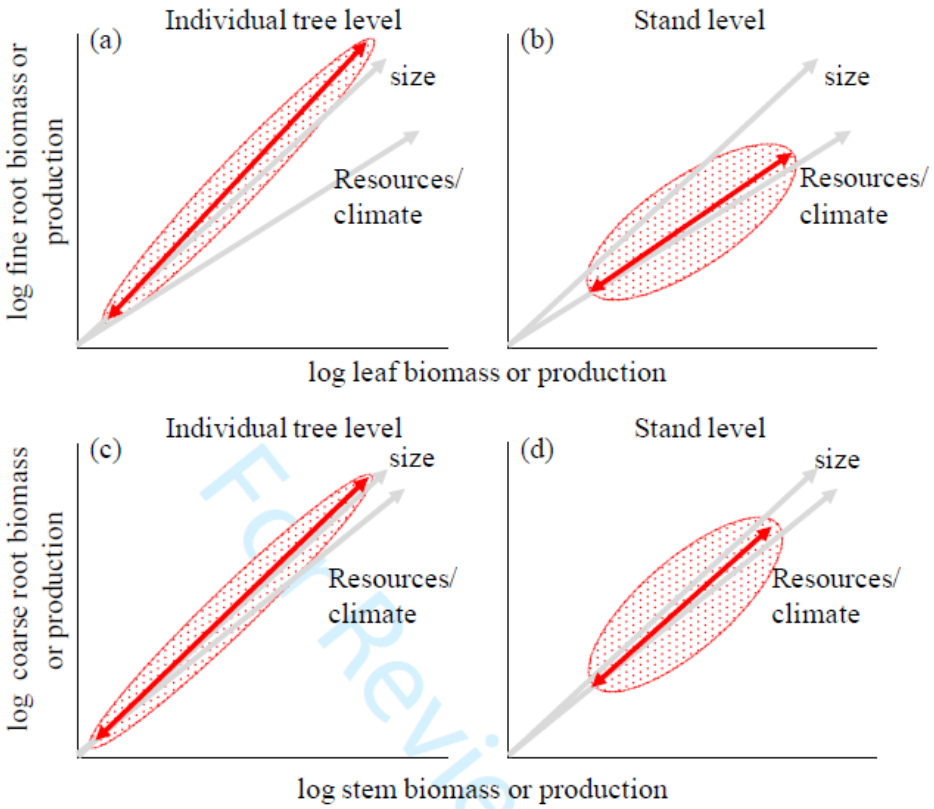

Fig. 3

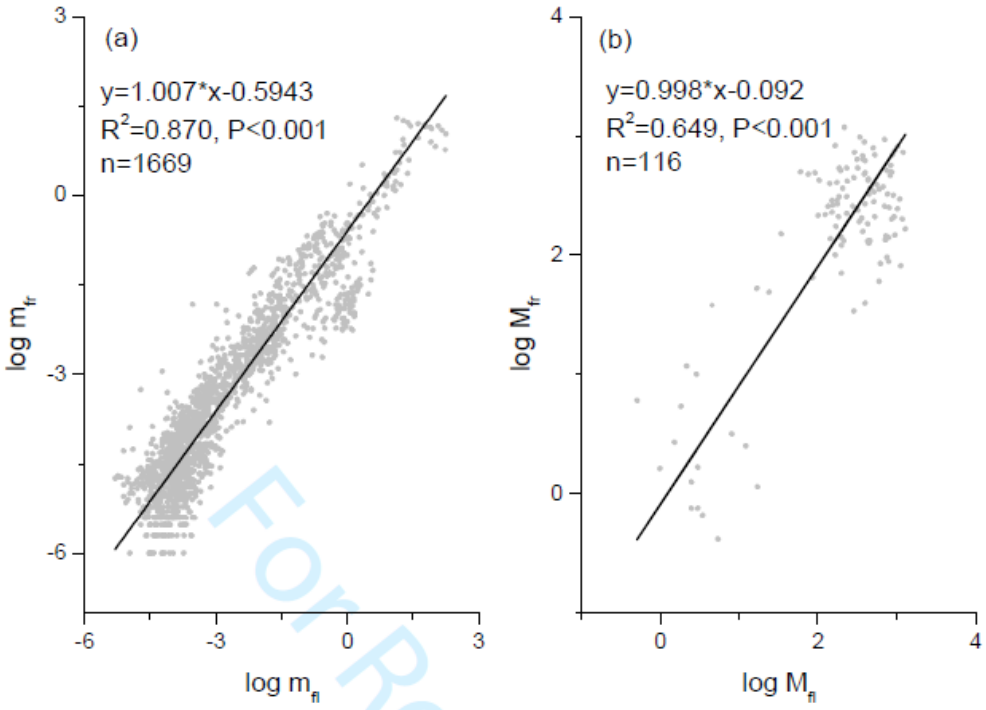

Fig. 4

792
793

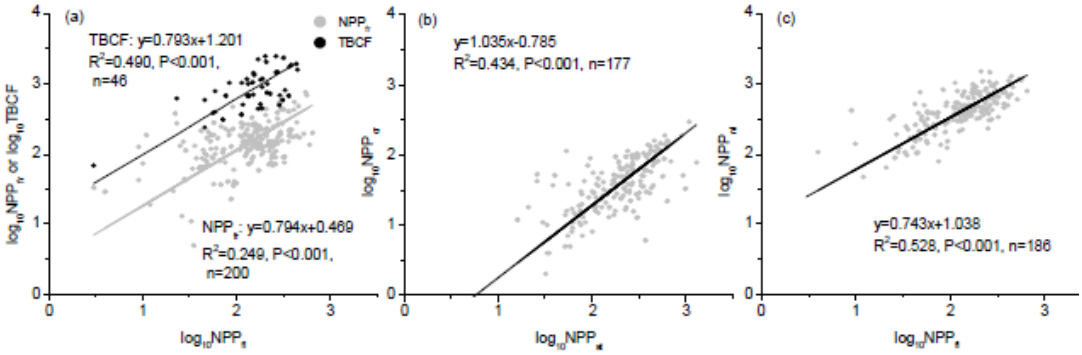
(a)
TBCF: y=0.793x+1.201
R²=0.490, P<0.001,
n=46
NPPn
TBCF
NPPp: y=0.794x+0.469
R²=0.249, P<0.001,
n=200
log10NPPn or log10TBCF
log10NPPp
(b)
y=1.035x-0.785
R²=0.434, P<0.001, n=177
log10NPPd
log10NPPp
(c)
y=0.743x+1.038
R²=0.528, P<0.001, n=186
log10NPPd
log10NPPp

Fig. 5

794
795

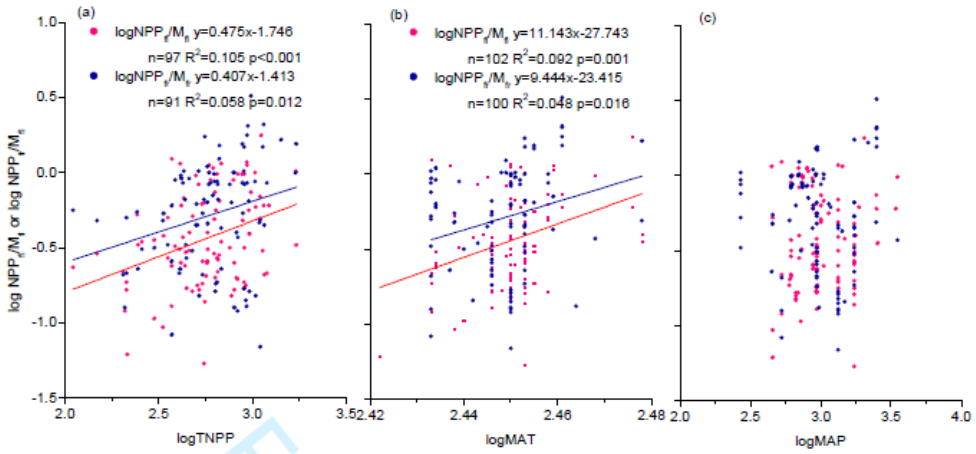
(a)
logNPP$_g$/M$_g$ y=0.475x-1.746
n=97 R^2=0.105 p<0.001
logNPP$_y$/M$_y$ y=0.407x-1.413
n=91 R^2=0.058 p=0.012
log NPP$_g$/M$_g$ or log NPP$_y$/M$_y$
logTNPP
(b)
logNPP$_g$/M$_g$ y=11.143x-27.743
n=102 R^2=0.092 p=0.001
logNPP$_y$/M$_y$ y=9.444x-23.415
n=100 R^2=0.048 p=0.016
logMAT
(c)
logMAP

Fig. 6

796

797

Table S1 The abbreviations and symbols used in this paper.

Abbreviations and symbols	Definitions
C	Carbon
GPP	Gross primary productivity
$iNPP_{cr}$	Coarse root production of an individual tree
$iNPP_{fl}$	The total leaf production of an individual plant
$iNPP_{fr}$	The total fine-root production of an individual plant
$iNPP_{nl}$	Non-leaf production of an individual tree
$iNPP_{st}$	Stem production of an individual tree
iTNPP	Total production of an individual tree
k_{fl}	Leaf turnover rate
k_{fr}	Fine-root turnover rate
MAP	Mean annual precipitation
MAT	Mean annual temperature
M_{fl}	Foliage biomass of a stand
m_{fl}	The total leaf mass of an individual tree
M_{fr}	Fine root biomass of a stand
m_{fr}	The total fine root mass of an individual tree
n_{fl}	The leaf number of an individual tree
n_{fr}	The number of fine root modules of an individual tree
NPP	Net primary production of a stand
NPP_{cr}	Coarse root NPP of a stand
NPP_{fl}	Foliage NPP of a stand
NPP_{fr}	Fine root NPP of a stand
NPP_{nl}	Non-leaf production of a stand
NPP_{st}	Stem NPP of a stand
NPP_{wd}	Woody NPP of a stand
RMA	Reduced major axis regression
sa_{fl}	The total leaf area of an individual tree
sa_{fr}	The total surface area of fine root modules of an individual tree
TBCF	Total belowground carbon flux of a stand
TNPP	Total net primary production of a stand

Table S2 Dataset used for analysis of scaling relationships at the stand level. See the Supporting Document

Table S3 Reduced major axis regressions between $\log_{10}$ transformed fine-root and foliage biomass both at the individual tree level and the stand level. m_{fr} and m_{fl}, fine root and leaf biomass of an individual tree (in kg C $stem^{-1}$); M_{fr} and M_{fl}, fine root and leaf biomass of a stand (in g C m^{-2}). CI is the 95% confidence interval.

Y	X	n	R^2	p	Slope	Lower CI	Upper CI	Intercept	Lower CI	Upper CI
$\log m_{fr}$	$\log m_{fl}$	1669	0.870	<0.001	1.007	0.990	1.025	-0.594	-0.650	-0.539
$\log M_{fr}$	$\log M_{fl}$	116	0.649	<0.001	0.998	0.894	1.114	-0.092	-0.355	0.170

802
803

Table S4 Reduced major axis regressions of $\log_{10}$ transformed components of net primary production of a stand (in g C m^{-2} yr^{-1}): fine root production (NPP_{fr}), foliage production (NPP_{fl}), stem production (NPP_{st}), coarse root production (NPP_{cr}), and non-leaf production (NPP_{nl}). RMA regression of $\log_{10}$ transformed total belowground carbon flux (TBCF) vs. NPP_{fl} was also listed for comparison with that of NPP_{fr} vs. NPP_{fl}. CI is the 95% confidence interval.

Y	*X*	*n*	R^2	*p*	Slope	LowCI	UppCI	Interc	LowCI	UppCI
log NPP_{fr}	log NPP_{fl}	200	0.249	<0.001	0.794	0.703	0.896	0.469	0.263	0.676
log NPP_{st}	log NPP_{nl}	177	0.434	<0.001	1.035	0.925	1.158	-0.785	-1.053	-0.518
log NPP_{nl}	log NPP_{fl}	186	0.528	<0.001	0.743	0.672	0.820	1.038	0.878	1.197
logTBCF	log NPP_{fl}	46	0.490	<0.001	0.793	0.639	0.983	1.202	0.823	1.580

804

805